ELECTRON-LENS TEST STAND INSTRUMENTATION PROGRESS*

T. A. Miller†, J. Aronson, D. M. Gassner , X. Gu, A. Pikin, P. Thieberger,
C-AD, BNL, Upton, NY, 11973, U.S.A.

Abstract

In preparation for installation of Electron Lenses [1] into RHIC, planned for late 2012, a working test stand (or "test bench") is in use testing the performance of the gun, collector, modulator, instrumentation and controls. While testing & operating the instrumentation, both progress and pitfalls were encountered. Results are presented from issues including ground loop signals generated by the DCCTs, static magnetic field interference, competing YAG screen illumination techniques, YAG crystal damage during beam operation, performance of the four quadrant beam scraper electrodes, and challenges in measuring beam current in conductors. Working knowledge and insight into each of these systems has been gained through difficulties leading to success. These insights are presented with supporting data and images.

INTRODUCTION

The major components of this test bench [2] include an electron gun (tested from 500ns to DC, 1.0A, 5keV) and an electron collector, normal & superconducting solenoids, a 5kV collector power supply (CPS) between gun & collector, and a 10kV fast modulator controlling the gun's anode. The system is equipped with pulse & DC current transformers at the gun and collector power supply, a beam profile monitor composed of both YAG crystal screen & camera and a pin hole Faraday cup intercepting the scanned electron beam, a four quadrant halo monitoring electrode array mounted just upstream of the collector, and an ion collecting Faraday cup electrode within the collector just downstream of the electron reflector [3]. As a complete overview of the diagnostics used was presented last year [4], details and experiences learned during recent system tests are presented in their respective sections below.

CURRENT MEASUREMENT

Beam current measurement is made with both DCCTs and pulse CTs placed on the conductors near the gun and collector connections, as shown in Fig. 1. The DCCT is a Bergoz IPCT-C-02 providing a resolution of 10uA over a range of 1-2000mA through a 2.7" aperture. It is sensitive from DC down to 100us pulses. The pulse CT is a Pearson model 6585 with 1V/A ratio, 50Ω output, 1.5ns rise time and a 0.3%/μs droop. This arrangement provides measurement of 1 – 5μs pulses without a noticeable droop and pulses longer than 100μs out to DC. However, ringing of the current pulse edges in the conductors obscures pulse shapes over the first 15μs.

* Work supported by B.S.A, LLC under contract No. DE-AC02-98CH10886 with the U.S. Department of Energy.
†tmiller@bnl.gov

Ground Current Problems in Pulsed Mode

As the 5kV CPS has its collector side grounded, a current transformer was installed in the ground connection in an attempt to measure ground return currents from beam loss to the grounded vacuum structure. Aside from the ringing on the pulses (discussed in the next section), a large distortion of the pulse was measured in the gun CT that was exactly compensated by an opposite distortion in the ground CT. Note that in the waveforms shown in Fig. 1, the summation (gold) of the gun (red) and ground (blue) current pulses exactly equaled that measured at the collector (yellow).

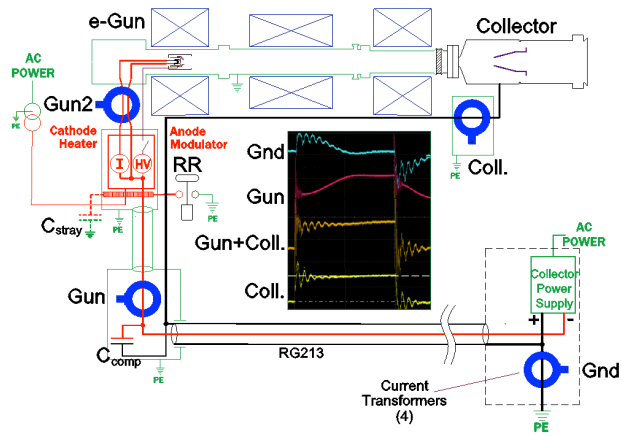

Figure 1: Current measurement system layout. Ground return currents found during pulsed beam operation impede attempts to measure beam loss currents.

The onset of the beam pulse current is believed to be supplied by stray capacitance of the floating instrument racks containing the gun power electronics on the cathode HV deck. This capacitance is shown in Fig. 1 as C_{stray}. An attempt to compensate for this undesired return path to the CPS via ground was made by installing a 5μF HV storage capacitor just before the gun CT, as shown in Fig. 1 as C_{comp}. This completely eliminated the ground coupled beam pulse current, except for the ringing, and brought agreement between the gun and collector CTs.

Ringing in Pulsed Beam Current Measurements

Initially, the fast edges (~50ns) of the beam pulse caused ringing in the currents measured by the gun, collector as well as ground CTs. Attempts were made to mitigate this ringing by adding RC filters (0.1μF, 50Ω) to either side of the 50Ω RG213 HV coaxial cable bringing power from the CPS to the cathode deck. However, these attempts have proved unfruitful.

Further attempts were made, such as providing a capacitive bypass around the ceramic break, shown in Fig.

ISBN 978-3-95450-119-9

1 at the interface between the green and black portions (ground and collector) of the accelerator. The effect was evident but only as a decrease in characteristic frequency of the ringing. The amplitude was unchanged.

New Gun CT

To improve measurement of the beam current pulse, a new pulse CT, labeled "Gun2" in Fig. 1, (also a Pearson 6585) was installed very close to the gun, and encircling both the cathode heater and HV common conductors, as the current is split between both conductors. The result, shown in Fig. 2 (cyan), evidences greatly reduced ringing in the measured pulse compared to the gun (red) & collectors (yellow) CTs.

Figure 2: Waveform from the new CT placed near the gun (blue – *increased amplitude*) installed just below the conductor feedthroughs; compared to those (red & yellow) placed ~1m away along the conductors.

The amplitude of the new CT (blue) is exaggerated compared to the original gun (yellow) and collector (red) traces by a factor of five. However, a much higher frequency component is observed and distorts pulses less than 1μs long. As a point of reference, the operating pulse length of the working Electron Lens [1] in pulse mode is to be ~0.5μs. Testing is planned with filtering.

Ground Loops

The current measurement system is equipped with a calibration current source, ILX Lightwave LDP-3811, capable of up to 0.5Adc at 10μA resolution and 0.1 – 1000μs in pulsed mode. With RG58 signal transport out to the CT enclosures and a 50Ω resistor in the loop through the CTs, a sharp calibration pulse can be propagated out to the CTs. This system is used for both offline calibration as well as system health checks during operation with beam.

At one point, the current measurement system was being tested while the electron gun was shut down. A noise of about 50mV with a repetitive nature was observed from the pulse CTs. This corresponds to a primary current of 50mA (1A/V). Our goal is to be sensitive to 1mA of beam current. At that time, most of the critical power supplies were shut down. Further investigation showed that the fundamental frequency of the noise was ~7kHz. This noise was also found on the calibration loop even with the calibration source disconnected. The source of the noise was identified when the noise disappeared with the removal of power to the DCCTs. The power supply is a linear supply and no such noise was found in the dc power.

The DCCT measures a DC current by its saturation of an AC-excited magnetic core. As the excitation oscillator runs at ~7kHz, the DCCT became suspect. However, it correctly measured calibration pulses within its response range. Adding to the confusion, this noise problem disappeared during the next run of the accelerator.

Due to the danger of high voltage floating platforms on which racks of electronics ride, safety-grounding relays are employed to ground these platforms when the machine is shut down. Ground loops often pick up noise that can be introduced into connected circuits. This system has several of these grounding relays. One such relay, labeled "RR" in Figure 1, is used to ground the HV cathode deck where the gun electronics are installed. It was later found that while this relay grounds the cathode deck, a large ground loop is formed from the CPS over its HV RG213 cable, through the CTs, to ground via the RR relay and back to the CPS via earth ground. This allowed the noise within the IPCT to be induced into this ground loop and measured by all the pulse CTs in the loop. This is why the problem disappeared when the machine was operated, as the safety ground relay (RR) was open.

Static Magnetic Field Interference

As the electron gun and entire beam transport are submersed in a solenoidal magnetic field, there are stray static magnetic fields that the instrumentation must deal with. The cross section of the solenoids can be seen in Figure 1 as blue rectangles around the beam pipe. A dc output offset of 156mV was observed in the DCCT installed in the gun circuit. This corresponds to 31.2mA (200mA/V), which exceeds the range of the zero offset correction on the DCCT. The static magnetic fields were therefore studied.

The stray magnetic field inside the CT enclosure was measured to be 14 Gauss, while simulations predict fields as high as 36 Gauss near the CTs in the final Electron Lens machine. A magnetic shield was made from a sheet of 0.030" thick Mu Metal and was made to wrap around the DCCT. The field inside the shield was measured to be ~1 Gauss. This reduced the dc output offset to 33mV. A design is being developed for a two-layer shield of iron and Mu Metal for the final Electron Lens installation.

YAG PROFILE MONITOR

One of the two beam profile monitors on this machine is comprised of a scintillating screen made of a Cerium doped single crystal YAG, 0.1mm thick mounted on a retractable holder just at the entrance of the collector. A GigE camera, AVT Manta G145B, fitted with a manual

ISBN 978-3-95450-119-9

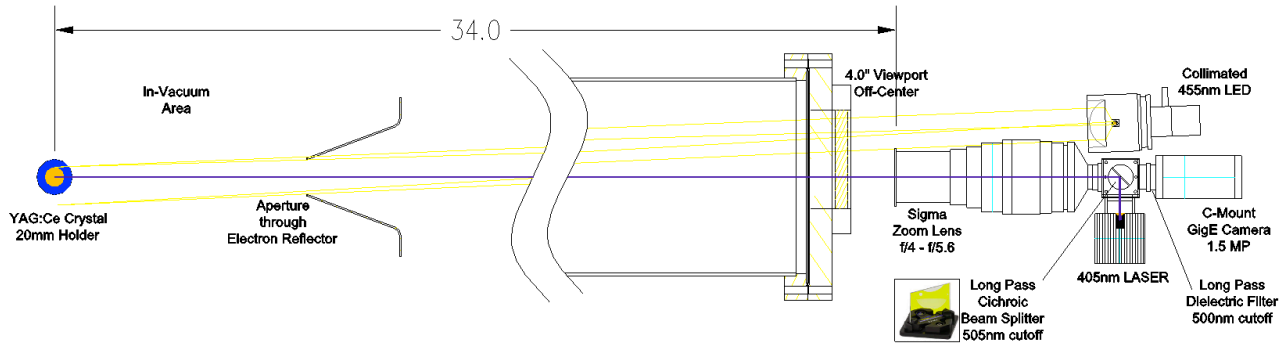

Figure 3: Layout of YAG profile monitor optics with UV laser, dichroic beam splitter, Sigma 70-300mm f/4-4/5.6 macro zoom lens, longpass filter, and GigE 1.5MPixel digital camera.

zoom lens, viewing the YAG screen through the hole in the electron reflector [4] and through a 4-inch viewport at the downstream extremity of the collector. The system is equipped with illumination light sources for inspection, discussed in detail below.

Lens Type Comparison

The original system design incorporated a specially assembled zoom lens [5] using Navitar lens components, as shown in Fig. 4. The advantage of this lens was its insensitivity to light outside of its field of view. It's disadvantage was a considerably small aperture; thus having a poor light gathering ability. Its forward aperture is only 25mm with a body length just over 300mm long and component cost totaling $1500.

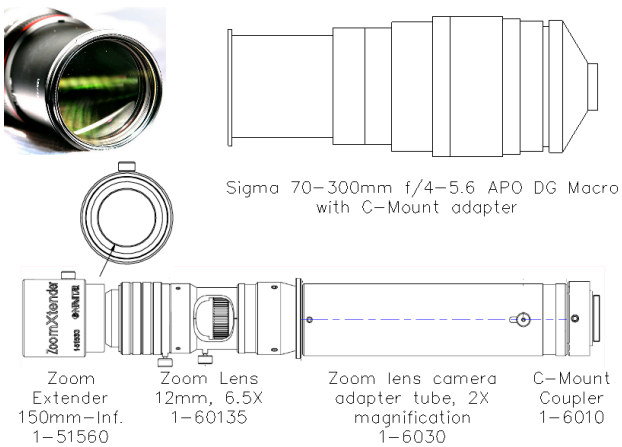

Figure 4: Two lenses compared. **Top:** Sigma f/4-f/5.6 lens with large aperture & compact body, **Bottom:** Navitar lens components with small aperture but good stray light rejection.

To avoid the YAG crystal's emission being degraded by elevated temperatures due to absorbed beam energy, an effort was made to find a lens with a larger aperture. A 70-300mm zoom lens by Sigma Corp., manufactured for the consumer SLR camera market and readily available for $200, was tested. The lens was mounted to the AVT Manta G-145B GigE camera, by Allied Vision Technologies; which has a Sony IXC285 2/3" type sensor (1.5 MPixels). Its forward aperture is about 50mm with a body length of 120 – 208mm depending on zoom. Although its minimum object distance (MOD) is 1.5m in macro mode, the distance between the lens and camera was increased in order to decrease the MOD; thus providing space for more optical components, as explained in the section on illumination techniques.

Tests with both lenses produced good resolution; where a resolution test of the Sigma lens setup measured 34µm (50µm being the goal.) The light gathering ability of this larger aperture lens was by far the benefit. Images of 200mA beam pulses taken with the Navitar lens required more than 3µS beam pulses with a gain of 33dB. The high gain produced very grainy images due to noise. Comparatively, the Sigma lens setup provided comparable beam images at 1µs and only 3dB of gain with a much less noise. The disadvantage of the Sigma lens is that it suffers severely from internal reflections within the lens. It is very sensitive to light from outside its field of view. Hence, illumination techniques previously possible with the Navitar lens, namely the flooding of light by an LED ring [5], is no longer possible. Moreover, with the increased diameter of the lens, less space is available for projecting light through the viewport alongside the lens. Figure 3 suggests that the viewport be mounted off center to accommodate this.

Illumination Techniques

White light illumination is provided by a collimated LED source [5]. Illumination at wavelengths that produce YAG fluorescence has been added. This provides a method to periodically test the health of the YAG crystal in situ. The optics layout in Fig. 3 shows the placement of a 500nm dichroic longpass beam splitter (1.1mm thick), Edmund Optics NT47-421, placed in the space between the camera and lens. This is used to project an enlarged 405nm laser spot onto the YAG crystal via the camera lens for focus determination and an in situ health check of the crystal. An image of the enlarged laser spot on the YAG crystal is shown in the upper left corner of Fig. 5. The 4mm laser oval laser beam is expanded by the camera lens to a 11mm spot on the YAG 1.3m away.

The dichroic beam splitter reflects the 405nm light into the optical path toward the YAG crystal and allows the broad spectrum YAG emitted light, ~500-700nm [7], to pass through to the camera while blocking any reflected

ISBN 978-3-95450-119-9

405nm light. A second layer of protection from UV light was added by placing a longpass dielectric filter, Thorlabs FEL0500, with 500nm cutoff, just in front of the camera.

Figure 5: YAG fluorescent illumination. **Left:** 405nm laser spot on YAG crystal via camera lens, pictured above laser module, heatsink, and beam splitter; and **Right:** YAG crystal (shown in red scale for contrast) flooded with 455nm light, pictured above the projection LED.

Initially, a 435nm longpass colored glass filter, Thorlabs FGL435S, was used to keep the UV light from reaching the camera. However, this filter fluoresced under the UV laser light and produced unwanted light from the surface of the filter. This led to the use of optics with dielectric coating where light with λ shorter than a cutoff is reflected instead of being absorbed.

The first dichroic beam splitter used, as shown in lower left corner of Fig. 5, was a thicker (3mm) model from Thorlabs. This thicker glass between the lens and camera first required a refocusing of the lens due to the longer effective path length, but finally degraded the resolution to a degree that appeared grossly out of focus. The much thinner 1.1mm optic from Edmund Optics was installed; yielding a resolution measurement of 34µm.

The laser used is a 5mW GaN diode laser, commonly found in Blue Ray players and now in laser pointers. It was purchased from Beam of Light Technologies [6]. This laser module is supplied with integrated current driver electronics, as shown in the lower left corner of Fig. 5 along with its heatsink mount.

YAG Beam Profile Measurements

Custom analysis software, developed in house, allows an image to be taken from the camera and stored in a project file. Tools are included to identify & mark the 20mm YAG screen border (for size calibration), to find the center of gravity of the beam spot, to overlay X, Y & θ axes (where θ is an arbitrarily selectable angle), and finally to generate three profile plots along each of the three axes. These are shown in Figure 6 along with the beam image they were taken from.

The beam profile images were initially taken using beam currents around 200mA and pulse widths of 12µs with a camera gain of 0dB. Once a problem with the gain control was fixed, the pulse widths were reduced to 3µs and a gain of 30dB was used (at the expense of higher noise). When the larger aperture Sigma lens was used the pulse widths were further reduced to 0.5µs with a gain of 3dB (with less noise), as in the case of the image in Fig. 6, but with a beam current of 725mA.

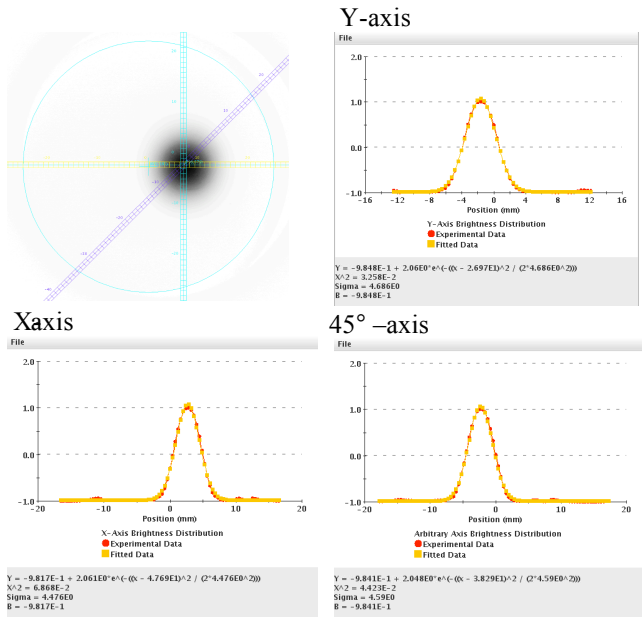

Figure 6: Profile of 10 mm beam spot on YAG with X, Y, and θ = 45° axes superimposed and the three beam profile graphs along each axis.

YAG Crystal Damage Incident

While propagating a 400 ~ 500mA beam of with a pulse width of 80µs and a rate of 1Hz, the YAG screen plunger was mistakenly inserted for about 3 pulses. The beam, measuring ~1cm on the YAG crystal, damaged the crystal to a point where it's single crystal structure was compromised. The normally transparent crystal sheet became opaque white. Photos in Fig. 7 show the damaged 30 x 0.1mm YAG crystal removed from its holder (1), a microscope photo of the damaged area (2), the damaged crystal exposed to 455nm light (3), and an image of a beam hitting high on the crystal showing the boundary between areas where the fluorescence capability was destroyed (4). Figure 7.3 shows an undamaged 5mm ring where the crystal was protected by the aluminum holder and still fluoresces as expected; where most of the damaged portion no longer fluoresces and reflects some of the incident blue light. The microscope images in Fig. 7.4 were taken of the heavily damaged area and are shown at a magnification of 15X with an inlay at 60X.

A study was done to estimate the penetration thickness for a 5keV electron beam incident on a YAG crystal

ISBN 978-3-95450-119-9

covered with a 100 nm thick aluminum layer. It was calculated that the entire energy of the beam is deposited in a surface layer only about 0.2 microns thick; leading to potential thermal shock damage due to sheer stresses that develop due to differential expansion of adjacent layers at different resulting temperatures. Ranges are rough estimates based on the so-called corrected Gruen formula. The temperature in this sublayer is predicted to have risen to 200°C during a 1μs pulse. This translates into a severe temperature gradient of 10^{10} °C/m.

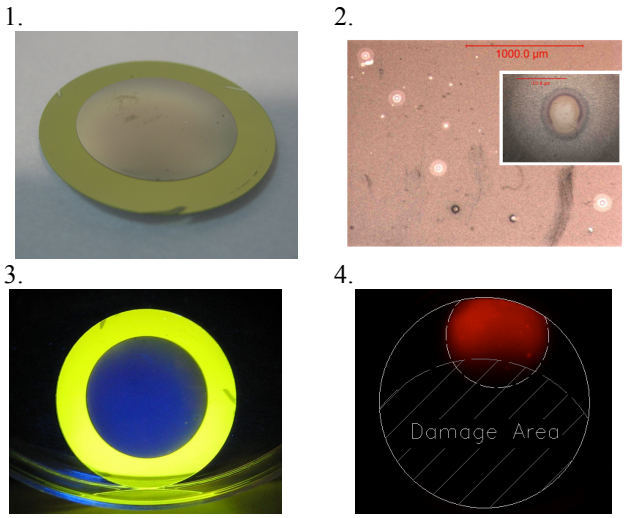

Figure 7: Damaged YAG **1.** damaged Al coated YAG; **2.** microscope image of damaged area; **3.** fluorescence of damaged crystal under 455nm light. **4.** top less-damaged area still partially sensitive to beam (20mm YAG screen boundary shown as solid line).

Plans for a Destructive YAG Test

In an attempt to find the non-destructive thermal limit affecting YAG fluorescence, the beam pulse length will be incremented while analyzing the YAG image profiles until the peak begins to flatten due to the thermal limiting of fluorescence. Then attempting to find a thermal limit causing permanent loss of fluorescence, profiles of YAG images will be analyzed while alternately taking images with the safe beam pulse length and an increasingly long beam pulse until the response of the crystal at the safe pulse length begins to be permanently altered.

FOUR QUADRANT HALO MONITOR

This instrumentation system includes a four quadrant scraper plate, or halo monitor. The four plates are circular quadrants with a 33.5mm diameter central aperture. Although conceived for the aid of steering & alignment as well as downstream beam loss detection, they have proved invaluable in determining machine parameters by clearly showing conditions of longitudinal beam oscillations between the gun and collector. Figure 8 shows the signals from the four plates during one such instance.

Figure 8: Signals from four quadrant halo monitor electrodes – signature of longitudinal beam oscillation.

CONCLUSION

With an installation of two electron lenses in RHIC planned by the end of 2012, the availability of the test bench approaches its end. What remains are a destructive test of a YAG crystal, the completion and testing of a pinhole scanning beam profile monitor (subject left for a future publication) and testing of a prototype BPM [8].

ACKNOWLEDGEMENTS

The authors would like to thank J. Hock, K. Hamdi, C. Liu, B. Sheehey. Special thank to Matthew Stetski for groundwork done during the summer of 2011 on the image analysis program. We appreciate the support from B. Schoepfer and members of the EBIS group as well as members of the controls group, especially A. Fatma, A. Fernando, L. Hoff, R. Olsen, & C. Theisen, and recognize the support of the Accelerator Components & Instrumentation Group, especially N. Baer, J. Carlson, T. Curcio, B. Johnson, J. Kelly, D. Lehn, J. Siano, D. Von Lintig, & A. Weston.

REFERENCES

[1] W. Fischer, et al, "Status of the RHIC Head-On Beam-Beam Compensation Project", Proceedings of PAC 2011, New York, NY, USA, THP055

[2] X. Gu, et al, "The E-Lens Test Bench for RHIC Beam-Beam Compensation", Proceedings of IPAC 2012, New Orleans, LA, USA, WEPPD084

[3] A. Pikin, et al, "Structure and Design of the Electron Lens for RHIC", PAC '11, New York THP100, p. 2309; JACow, https://www.jacow.org

[4] D. Gassner, et al, "RHIC Electron Lens Test Bench Diagnostics", DIPAC 2011, Hamburg, Germany, MOPD04, p. 38; JACoW, https://www.jacow.org

[5] T. Miller et al, "RHIC Electron-Lens Beam Profile Monitoring" BIW 2012, Newport News, VA TUPG039

[6] Beam of Light Technologies, 10117 SE Sunnyside Rd. Suite F, MB 324, Clackamas, OR 97015 http://www.z-bolt.com/

[7] Y. Zhu, et al, "Investigation of the Optical Properties of YAG:Ce Phosphor", Lighting Research Center, Rensselaer Polytechnic Institute, 21 Union St. Troy, NY 12180

[8] P. Thieberger, et al, "Conceptual Design of a High Precision Dual Directional Beam Position Monitoring System for Beam Crosstalk Cancellation and Improved Output Pulse Shapes", BIW 2012, Newport News, VA MOPG024

ISBN 978-3-95450-119-9